Numerical analysis of 3D mass diffusion in random (nano) composite systems: Effects of polydispersity and intercalation on barrier properties

Sarra Zid, Matthieu Zinet, Eliane Espuche

Numerical Analysis of 3D Mass Diffusion in random (Nano) composite Systems: Effects of Polydispersity and Intercalation on Barrier Properties

Sarra ZID, Matthieu ZINET, Eliane ESPUCHE*

Univ Lyon, Université Lyon 1, CNRS UMR 5223, Ingénierie des Matériaux Polymères, F-69622 Villeurbanne, France

*to whom correspondence should be addressed
e-mail: eliane.espuche@univ-lyon1.fr

Abstract

Nanocomposite systems show promise as barrier materials for a wide range of applications. However, the enhancement of barrier properties requires a better understanding of the relationship between the system structure and the desired properties. The aim of the present study is to discuss first the effect of fillers size polydispersity on gas barrier properties through a step-by-step approach based on three-dimensional finite element modeling (FEM). Secondly, dispersions of monodisperse and polydisperse stacks are investigated coupled with a sensitive study of interplatelet diffusion effect on the overall diffusivity considering a wide range of diffusion coefficient values in the interplatelet area. The specificity of the developed model is its ability to account for interplatelet diffusion for a large range of fillers dimensions.

Keywords: diffusion, modeling, polydisperse, intercalation, barrier properties

1. Introduction

In the past decades, there has been specific interest in nanocomposite materials because of their applications in various fields, especially for gas barrier application. An increase of the barrier properties is expected from the addition of impermeable lamellar nanofillers to the polymer matrix thanks to an increase of the gas diffusion path. Different experimental, analytical and numerical studies have been carried out to investigate the dependency of this tortuous effect and resulting barrier properties on morphological factors such as the filler content or aspect ratio[1–8]. In these studies, it is usually considered that all dispersed objects have the same dimensions[2,3]. However, the nanocomposite morphology is often more complex. Several studies have underlined the coexistence of dispersed objects with different aspect ratios in nanocomposites prepared from a single nanofiller type due to the difficulty to achieve complete exfoliation of the platelets[9–12]. Picard et al.[13] showed that in PA6/montmorillonite nanocomposites the coexistence of exfoliated structures and small filler stacks (less than 5 sheets per stack) was not detrimental to barrier properties. This result, that could appear surprising with respect to commonly used Nielsen law [8], was explained by the low amount and low width of the stacks. Thus, the small decrease of mean filler aspect ratio was compensated by the increase of the impermeable volume fraction, the volume occupied by the stacks being considered as impermeable.

The effect of the polydispersity of the filler aspect ratios on barrier properties has been modeled in several works[14,15]. In these studies, the considered fillers have the same thickness but generally differ by their length. The analytical model developed by Lape et al.[14]evidenced that the barrier properties are better improved when fillers are larger. Moreover, Chen et al.[15] developed a 2D numerical model based on the Boundary Element Method (BEM) through which they confirmed the interest of filler size polydispersity for improved barrier properties. As already mentioned, in all these studies, the dispersed objects consisted of individual fillers with the same thickness but different lengths. On the other hand, some works focused on the effect of filler stacks on gas transport[16,17]. The stacks dispersed in the matrix had the same size and they were usually considered as impermeable phases. Only few authors investigated the influence of possible gas diffusion in the interplatelet space on the overall gas transport properties. By considering the gas diffusion rate in the interplatelet space similar to that in the matrix, Nazarenko[18] found that the contribution of the interplatelet diffusion on the overall transport was negligible. An extension of the model proposed by Nazarenko was derived by Greco and coworkers[19,20] with the aim to discuss the impact of different diffusion rates in the interplatelet space. Through their numerical approach, Greco et al. showed that diffusion in the interplatelet space is quite relevant especially for high values of the space inside stacks. It is noteworthy that in all these previous works the platelet stacks dispersed in the matrix were all of the same sizes. According to our knowledge, no modeling study investigated the impact of stacks with polydisperse sizes on the gas transport properties.

The aim of the present study is to discuss the effect of the filler size polydispersity on gas barrier properties through a step-by-step approach based on three-dimensional finite element modeling (FEM). In the first part, systems filled with polydisperse single platelets (*i.e.* same thickness but different diameter distributions) are compared with monodisperse systems. In the second part, dispersions of monodisperse stacks and polydisperse stacks are investigated. In order to assess the effect of interplatelet diffusion, a sensitivity study is carried out considering a wide range of diffusion coefficient values in the interplatelet area. It should be kept in mind that throughout this study, random spatial dispersion of the fillers (or stacks) has been assumed in order to be as representative of the actual systems as possible.

2. Modelling Methodology

2.1. Geometry

The geometric modeling of the nanocomposite systems is based on a three-dimensional representative volume element (RVE) approach. The parallelepipedic simulation domain representing the RVE has dimensions L_x, L_y and L_z in a Cartesian coordinate system (x,y,z), with z the overall diffusion direction. As in a previous work by the present authors[1], fillers are modeled as three-dimensional disks (diameter D, thickness e). The choice of the discoidal filler shape was based on literature[21] because of its representativeness of platelet-like nanofillers. Two types of geometric configurations have been considered:

- the first type of configuration consisted of dispersions of single impermeable disks randomly positioned in the matrix and oriented normally to the overall flux direction z. The disk size can be either monodisperse or polydisperse. The random positioning of disks in the computational domain was generated using a JAVA algorithm coupled with the commercial

finite element package COMSOL Multiphysics. This algorithm contains conditions that ensure non-overlapping of the generated disks.

- the second type of configuration consisted in dispersions of stacks of three impermeable disks, randomly positioned and oriented in the polymer matrix using the same generation algorithm. As in the first type of configuration, the disk size can be either monodisperse or polydisperse.

In the whole study, the disk thickness was assumed to be 2 nm and the mean diameter value $\overline{D}$ was targeted to 60 nm. The filler aspect ratio α was defined as the ratio between the diameter and the thickness. A target value of the filler volume fraction was specified as an input parameter of the distribution generation algorithm. However, the actual volume fraction f of the generated distribution was calculated through a volume integration of the matrix domain after generating the geometry and was varied between 1% and 14%. The computational domain contains a sufficient number of fillers through which well-aimed results could be obtained (200 - 264 dispersed fillers with and without stacks).

2.2. Physical equations

The mass diffusion process in stationary regime was modeled according to Fick's second law without mass source[1]:

$$\boldsymbol{\nabla \cdot \left(-D_{ij} \nabla c_i\right) = 0} \qquad (1)$$

where c_i is the molar concentration of the permeating specie *i* (mol.m^{-3}) and D_{ij} is the mass diffusion coefficient of permeating specie *i* in medium *j*. In the present study, the diffusion coefficient of permeating specie in the neat matrix was chosen as D_0 = 10^{-12} m²/s.

The finite element method is used to solve the mass diffusion equation in the matrix domain with the following boundary conditions:

- concentration boundary conditions were imposed on the upper and lower faces of the simulation domain: c_1 = 1000 mol.m^{-3}; c_2 = 500 mol.m^{-3}. The matrix diffusivity is considered constant and not concentration-dependent, meaning that concentration values chosen as BCs for the upper and lower faces have rigorously no effect on the effective diffusivity calculated in this study;

- since disks are impermeable to mass diffusion, no-flux boundary condition was imposed on all filler-matrix interfaces;

- for symmetry reasons, no-flux boundary conditions were applied on the lateral faces of the simulation domain.

2.3. Numerical analysis

An unstructured mesh consisting of tetrahedral linear elements in order to provide accurate results was adopted in this work[1]. It has been verified that the number of mesh elements is sufficiently high not to affect the obtained results (*e.g.* for 200 disks generated in the RVE, the number of mesh elements is about 126360). The solution of the boundary value problem yields the molar concentration field of the permeating specie *c*(*x,y,z*). Finite element solutions were obtained using

the commercial package Comsol Multiphysics (version 5.4, DELL computer with i3 processor and 8 Go of RAM). The computational time was between 1 and 5 min. The mass flux vector field of the permeating specie can be calculated from the concentration field:

$$\vec{N}(x,y,z) = -D_0 \vec{\nabla} c(x,y,z) \quad (2)$$

and the overall effective diffusivity is given as follow:

$$D_{eff} = \frac{\overline{N_z} L_z}{c_1 - c_2} \quad (3)$$

where $\overline{N_z}$ is the average mass flux of the permeating specie across a plane section *S* normal to *z*-direction and located at $z = z_0$ within the unit cell:

$$\overline{N_z} = \frac{1}{L_x L_y} \iint_S N_z(x,y,z_0) dx dy \quad (4)$$

assuming that N_z is the *z*-component of the mass flux vector.

In the current work, relative effective diffusivity, defined as the ratio D_{eff}/D_0, is considered the most convenient parameter to characterize and compare the enhancement of barrier properties in the various studied systems. It has been shown through a previous work[1] that it doesn't depend on the neat matrix diffusivity value D_0.

3. Results and Discussion

3.1. Effect of filler aspect ratio polydispersity on the overall diffusivity

This section focuses on the effect of filler aspect ratio polydispersity on nanocomposite barrier properties. For this purpose, simulations were conducted for different generated distributions in order to compare their effect on the overall diffusivity. For the sake of clarity, the generated distributions are described first, then the obtained results are discussed and compared to existing models from literature.

3.1.1. *Monodisperse distribution*

Monodisperse distributions have been generated according to the following method: single disks having a fixed diameter value $D = 60$ nm corresponding to an aspect ratio value $\alpha = 30$ were positioned randomly on 4 layers separated by 1 nm of the polymer matrix, each. The developed generation algorithm ensured that disks did not overlap in a given layer (Fig. 1).

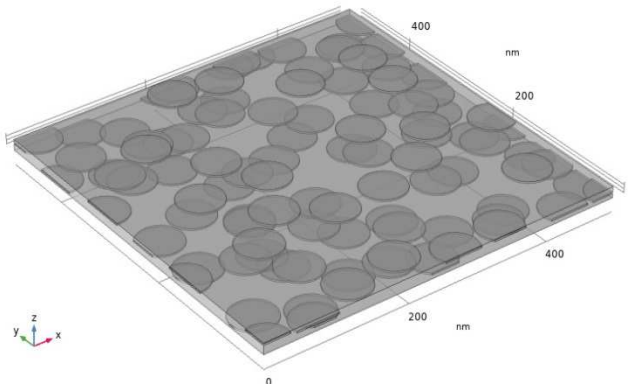

Figure 1 : Geometrical model of monodisperse system

3.1.2. Polydisperse distributions

Nanocomposite systems could have various filler size distributions. In this section, three different types of distributions are presented where the polydispersity was controlled. For each type of distribution, three dispersions were randomly generated in order to verify the repeatability of the method.

- Polydisperse uniform distribution

In order to generate a polydisperse system with uniform size repartition in a given range, the generation algorithm randomly picks an equiprobable random value of the disk diameter in the specified range (20 – 100 nm in the present case) and attempts to position the disk at a randomly chosen position. If no overlapping occurs, the disk is actually inserted. Otherwise, the disk is discarded and a new disk with new random diameter and position is generated. The process is repeated as many times as needed to attain the desired number of disks in the RVE. Due to this process, it is expected that the actual diameter distribution slightly deviate from the ideal uniform distribution, since small disks are generally easier to position than large disks. For a total number of 200 generated disks in the RVE, the actually obtained distributions of disk size for an average disk aspect ratio $\bar{\alpha} = 30$ (corresponding to an average diameter $\overline{D}$ = 60 nm) is presented in Fig. 2.

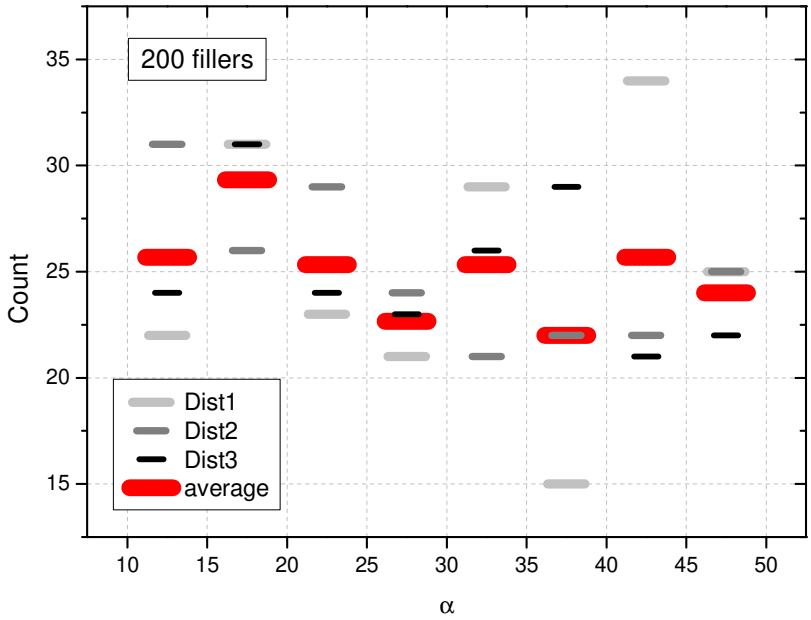

Figure 2 : Disk size distribution for three different polydisperse uniform dispersions ($\bar{\alpha} = 30$); resulting averaged distribution

- Polydisperse Gaussian distribution

Polydisperse systems with Gaussian size distribution were generated. This type of distribution has the following probability density function (PDF):

$$\phi = \frac{1}{\sqrt{2\pi}\sigma} e^{-\frac{(D-\bar{D})^2}{2\sigma^2}} \qquad (5)$$

where $\bar{D}$ is the diameter mean value and σ the diameter standard deviation. Two different standard deviation values σ = 1 (narrow distribution) and σ = 10 (wide distribution) were chosen, in order to stay in the same range of individual D values as for the uniform distribution. For each σ value, three different dispersions were generated. The obtained diameter distributions are plotted and compared to Gaussian fits of these distributions on Figs. 3 and 4 for σ = 1 and σ = 10, respectively. It appears clearly that for both σ values, the actually obtained distributions (represented by the histograms) were quite close to Gaussian distributions.

- Polydisperse "specific" distribution (derived from Gaussian distribution with large standard deviation)

The aim was to generate target Gaussian distributions with a mean aspect ratio value $\bar{\alpha}$ = 30 and a larger standard deviation value σ = 20. However, due to the overlapping management process described earlier, the generation algorithm tends to discard the larger disks (whose diameters belong to the upper tail of the Gaussian) more frequently and thus to favor the smaller disks. Consequently, the mean aspect ratio values of the actually obtained distributions ($\bar{\alpha}_1 = 22.3$; $\bar{\alpha}_2 = 22.4$ and $\bar{\alpha}_3 = 21.7$) are significantly smaller than the target value $\bar{\alpha} = 30$. Moreover, the obtained distributions clearly deviate from true Gaussian distributions and present a truncated aspect in the lower tail (Fig. 5).

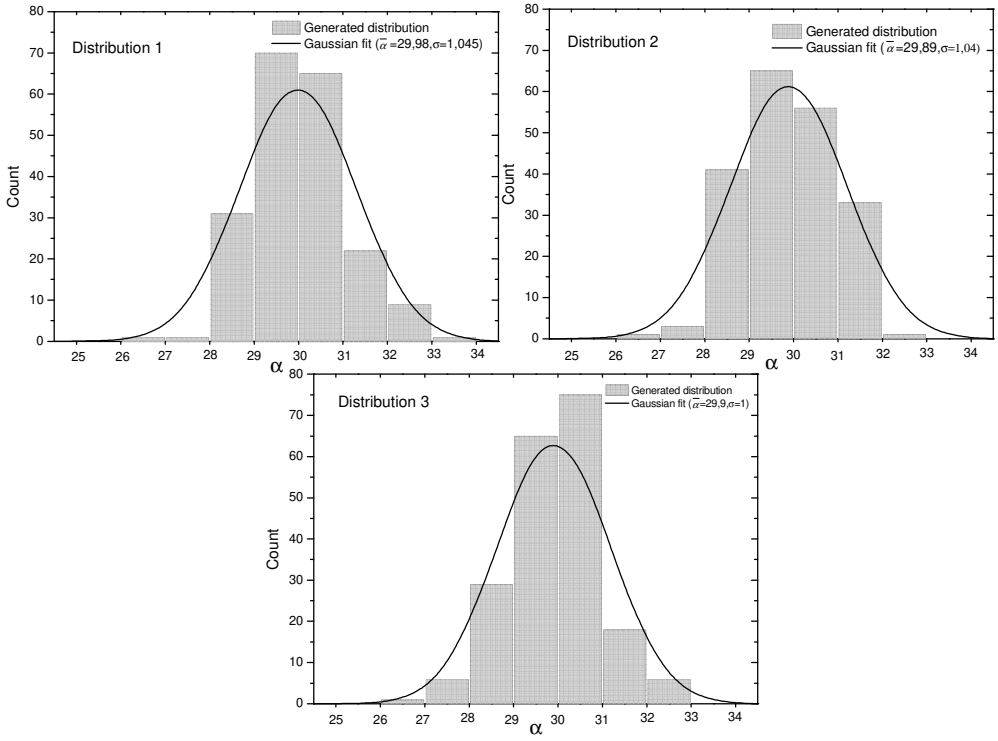

Figure 3 : Disk size distribution actually generated for target values of Gaussian parameters $\bar{\alpha}$ = 30 and σ = 1

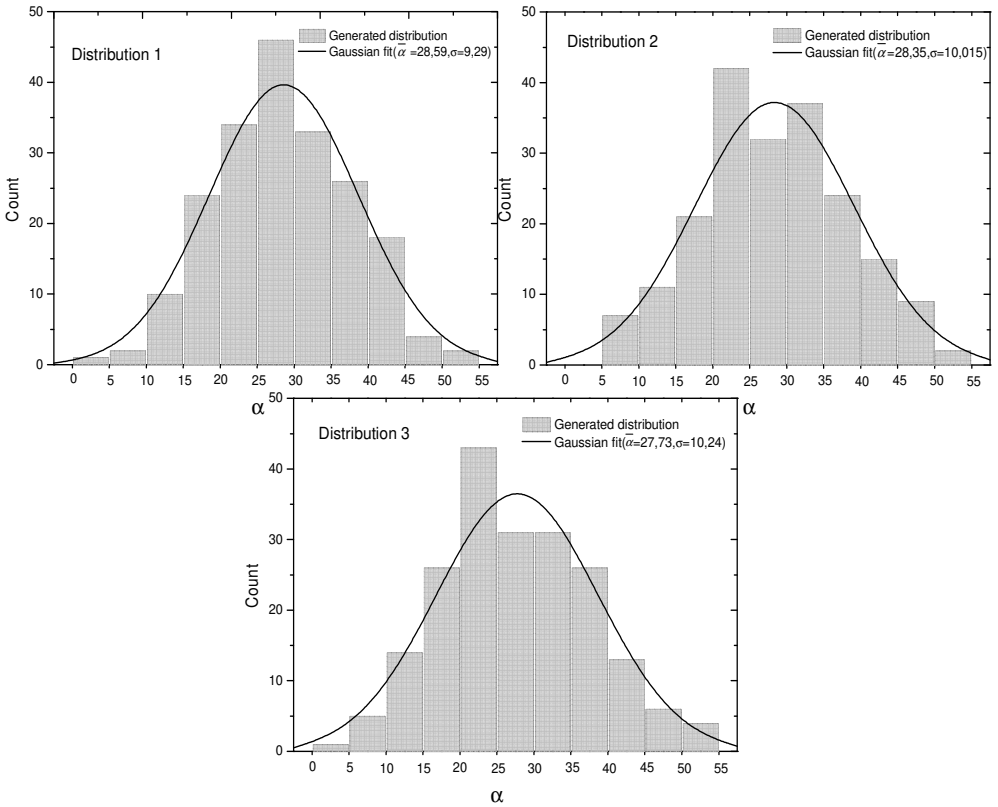

Figure 4 : Disk size distribution actually generated for target values of Gaussian parameters $\bar{\alpha}$ = 30 and σ = 10

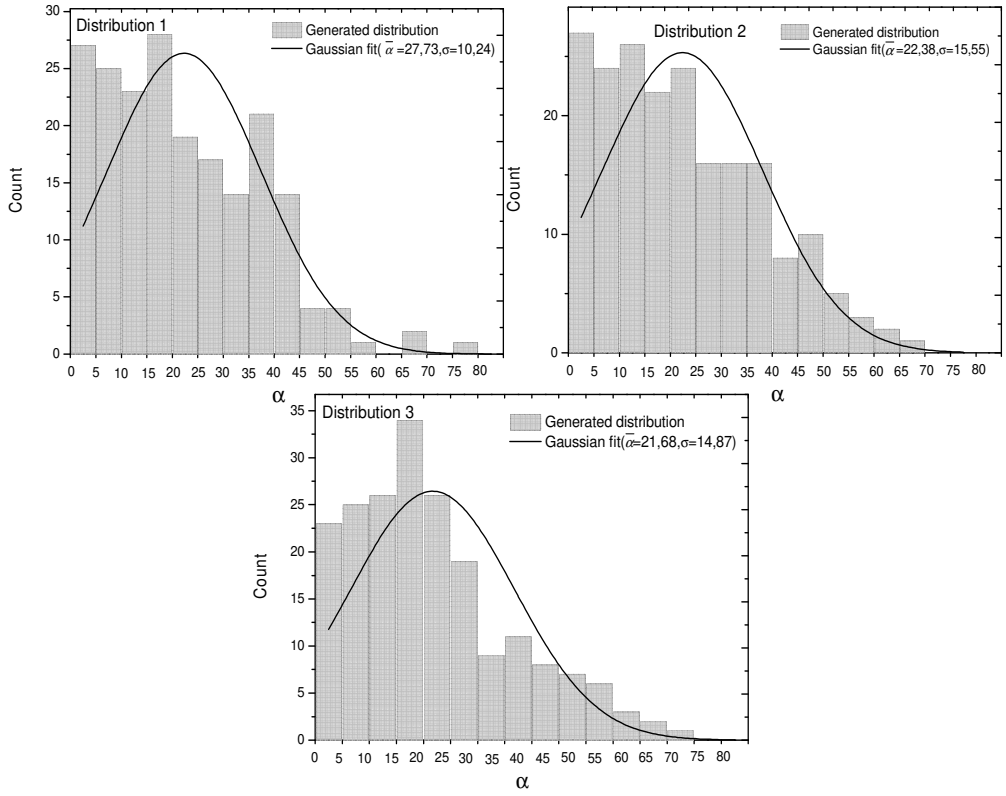

Figure 5: Disk size distribution actually generated for target values of Gaussian parameters $\bar{\alpha}$ = 30 and σ = 20

3.1.3. Comparison of barrier properties

An objective of this study is to clarify which type of filler dispersion is the most efficient in the enhancement of nanocomposite barrier properties. Hence, in this section, relative effective diffusivity (D_{eff}/D_0) results from finite element simulations of the different studied configurations are compared. Moreover, the numerical results are compared to Lape et al.[14] analytical equation, for which filler size also follows a Gaussian distribution:

$$\frac{D_{eff}}{D_0} = \frac{1-f}{\left(1+\left(\frac{f}{3e\bar{D}}\right)\left(\frac{\bar{D}^2}{4}+\sigma^2\right)\right)^2} \quad (6)$$

where f is the filler volume fraction, e the disk thickness, $\bar{D}$ the disk average diameter and σ the diameter standard deviation. Figure 6 plots the relative diffusivity predicted by FEM for the monodisperse and Gaussian polydisperse systems, as well as Lape analytical model's predictions for the Gaussian polydisperse systems (σ =1 and 10). The standard deviation (ε) has been determined for the lowest and highest filler volume fractions considered in this work. It is less than 0.01 and can thus be considered as negligible in comparison with the relative diffusivity evolutions observed as a function of the filler dispersion type.

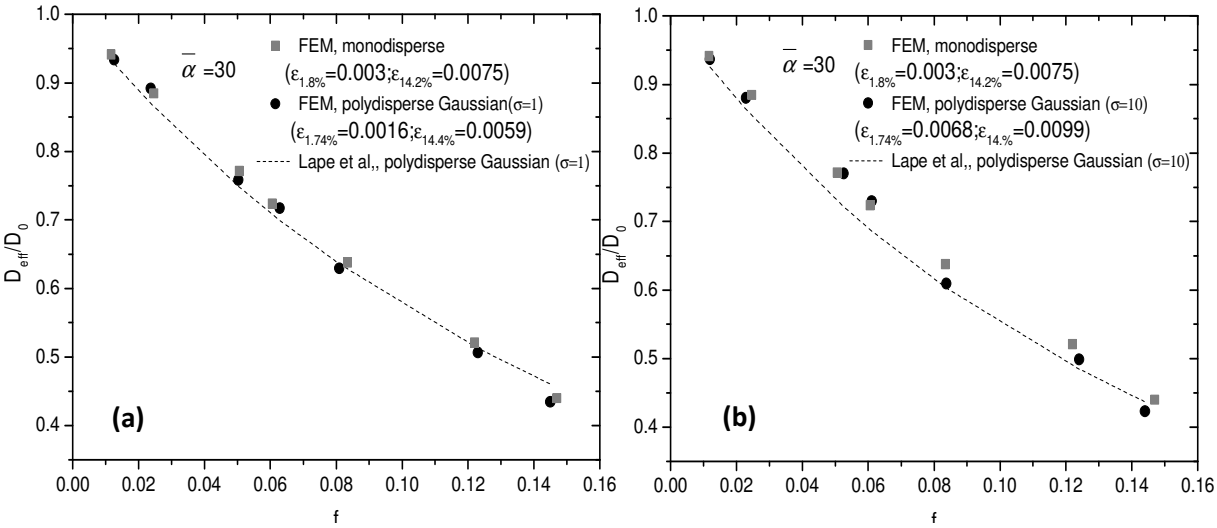

Figure 6: Relative effective diffusivity vs. filler volume fraction for monodisperse and polydisperse Gaussian systems (σ = 1 **(a)** and σ = 10 **(b)**): FEM predictions and Lape et al.[14]model

It can be noticed that results from the present simulations are in good agreement with Lape's model predictions. Moreover, when σ is increasing, the deviation between polydisperse and monodisperse systems is slightly increasing too. Lape et al.[14] showed that an increase in polydispersity (i.e. an increase in σ) implies a decrease in diffusivity, which is consistent with our calculations.
In a next step, the comparison has been extended by taking into account the polydisperse uniform distribution and the polydisperse specific distribution described previously (Figure 7).

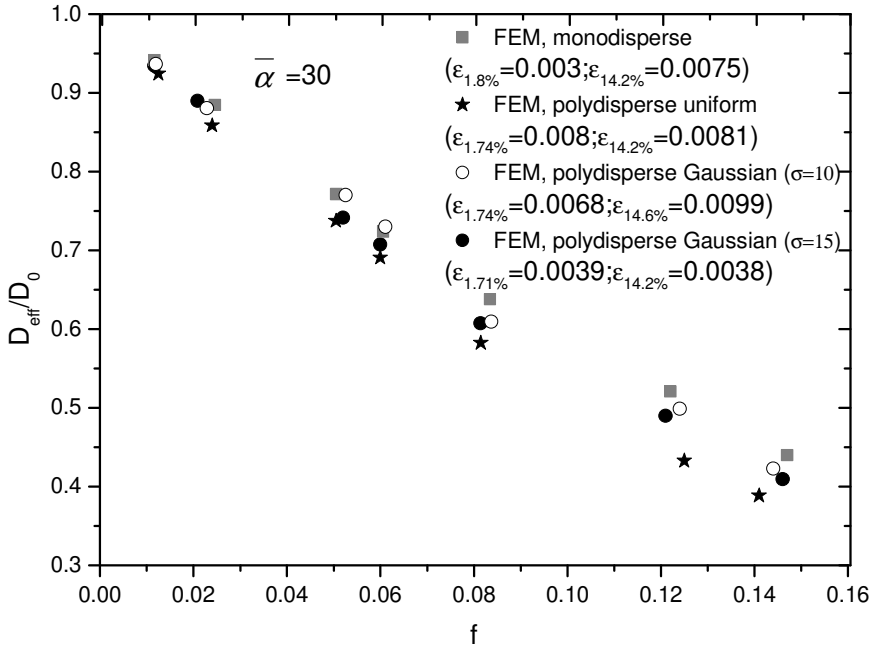

Figure 7: Relative effective diffusivity vs. filler volume fraction for monodisperse, polydisperse uniform and polydisperse Gaussian systems: FEM predictions

It appears clearly that although relative effective diffusivity always decreases as fillers volume fraction increases, the type of distribution does have a significant effect. Indeed, the lowest diffusivity values were obtained in the case of uniform polydispersity. It has been shown in our

previous work [1] that barrier properties enhancement is correlated to the projected area ratio for penetrating molecules which was defined as the ratio of the projected area of the matrix phase on a plane normal to the diffusion direction z and the total projected area of the RVE. In this case, this factor, denoted k_i, was calculated for three different cases of size distributions (monodisperse (k_1), polydisperse uniform (k_2), and Gaussian σ = 10 (k_3)). The values of k_i reported in Fig. 8 are the average values calculated from 3 different dispersions for each size distribution. As it can be observed, the lowest value of the projected area ratio is obtained for the polydisperse uniform configuration which is in adequacy with the obtained numerical diffusivity results.

Furthermore, a comparison of the results for the Gaussian distribution shows a slightly better decrease in relative effective values in the case where σ = 15 compared to σ = 10. One should remember that, when the standard deviation is targeted to σ = 20, the generated distribution is not perfectly Gaussian and the actual standard deviation is about σ = 15. Thus, In all cases, relative effective diffusivity values are smaller than the monodisperse case; this is consistent with Chen et al.'s 2D simulation results[15].

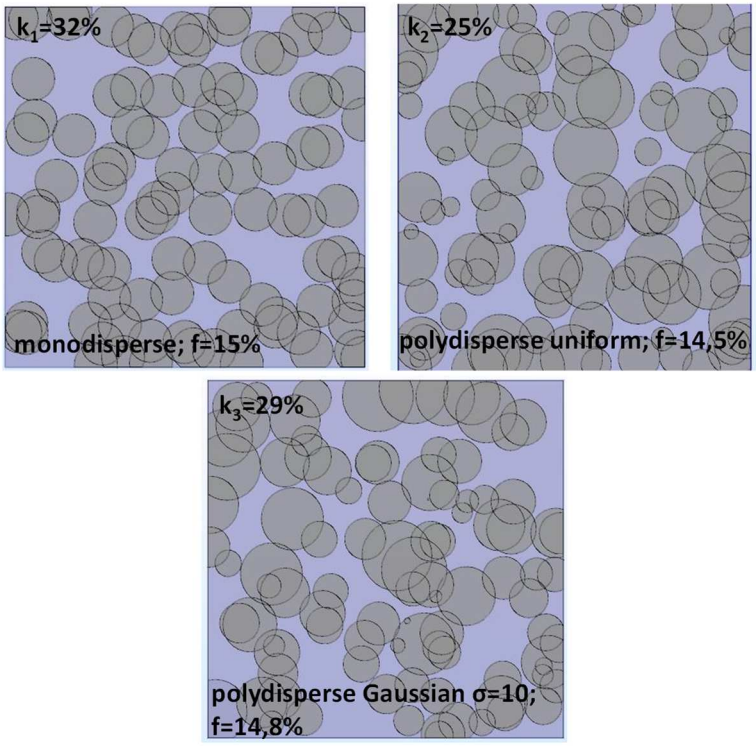

Figure 8: Representative volume element (*z*-direction view) of three types of filler dispersion for similar filler volume fraction

3.2. Effects of intercalation on the effective diffusivity

Fillers present in nanocomposites (graphene, montmorillonite) often have an intercalated structure[10–13,22]. Hence, investigating the effects of filler stacking on diffusion mass transfer is an indispensable step to understand the barrier properties of such nanocomposite films. In the previous section, the size polydispersity of the dispersed objects (single fillers) was taken into account by the variation of the disk diameter. In the case of nanocomposites prepared from lamellar nanofillers, the size polydispersity is related to the presence of nanofiller stacks[13]. In this section, a step-by-step analysis is presented, covering monodisperse and polydisperse stacks and considering the most efficient size distributions evidenced previously.

3.2.1. *Effects of stacking and polydispersity*

First, an analysis has been conducted in order to examine to what extent the presence of stacked fillers affects the barrier properties in comparison to an exfoliated system with a similar volume fraction. Each stack was modeled as a superposition of three identical disks (diameter *D*, thickness *e*). The interplatelet spacing, *i.e*. the gap between two adjacent disks in a stack, e_{inter}, was assumed identical (e_{inter} = 1 nm) for all stacks. The stacks were randomly positioned in the simulation domain and oriented perpendicularly to the gas flow. The *z*-dimension of the simulation domain corresponds to four layers of stacks. Two examples of generated stacks dispersions are shown in Figure 9. In all cases, the generation algorithm ensured non-overlapping of stacks. The following distributions have been generated and diffusion mass transfer has been numerically simulated for various volume fractions using the methodology presented in section 2:

- monodisperse distribution: identical stacks (*D* = 60 nm, *e* = 2 nm, e_{inter} = 1 nm);
- polydisperse uniform distribution (diameter range : 20-80 nm, $\overline{D}$ = 60 nm, *e* = 2 nm, e_{inter} = 1 nm);
- polydisperse Gaussian distribution (average diameter $\overline{D}$ = 60 nm with a standard deviation σ = 10, *e* = 2 nm, e_{inter} = 1 nm);

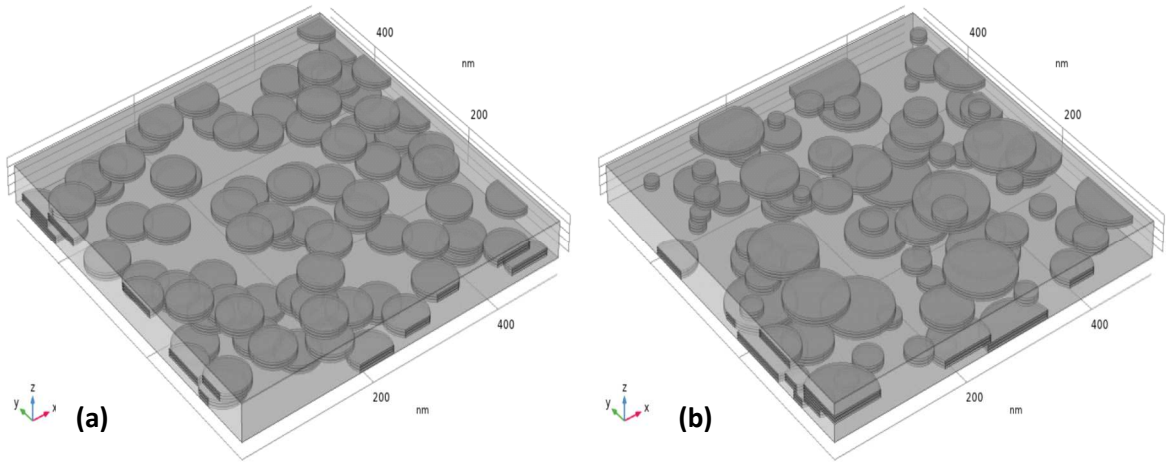

Figure 9: Example of 3D simulation domain of intercalated nanocomposites; **(a)** Monodisperse stacks **(b)** Polydisperse stacks (uniform distribution)

The effective relative diffusivity values predicted for the three types of intercalated dispersions have been reported in Fig. 10 and compared to the results obtained in section 3.1.3 for the exfoliated structures. As expected, the relative effective diffusivity is a decreasing function of fillers volume fraction. It is noteworthy that whatever the filler volume fraction, the relative diffusivity is lower for the exfoliated dispersions than for intercalated ones. This observation can be assigned to the tortuosity effect. Indeed, for a given value of the filler volume fraction, the total projected area of the impermeable phase is larger in the case of single disks than in the case of stacks. According to our previous study[1], this factor can be related to the tortuous path a diffusing molecule have to follow due to the presence of the impermeable phase. More specifically, for the intercalated systems, it can be noticed that the highest relative diffusivity values are obtained for monodisperse stacks while the

lowest relative diffusivity values are recorded for the polydisperse uniform distribution of stacks. Thus, the trends observed for exfoliated dispersion are also valid for intercalated dispersion.

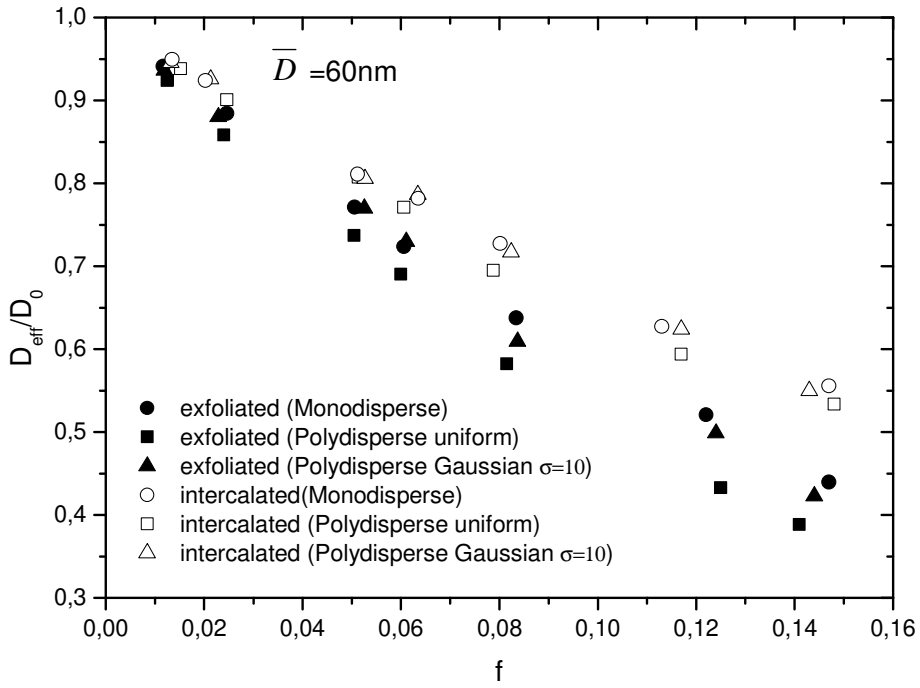

Figure 10 : Comparison of effective relative diffusivity predicted by FEM for exfoliated and intercalated systems as a function of filler volume fraction

3.2.2. *Influence of the interplatelet space characteristics (spacing, diffusivity)*

In order to investigate the potential contribution of the interplatelet space to overall diffusion, monodisperse systems composed of 3-disks stacks with a fixed diameter were considered. The stacks were randomly positioned in the polymer matrix. Moreover, they were randomly tilted with angles ranging between 0° and 30° around both *x* and *y* axes, as shown in Fig. 11. The disk thickness was fixed to e = 2 nm whereas the disk diameter could be chosen in the range [20 nm - 100 nm]. The interplatelet spacing e_{inter} was varied between 1 nm and 10 nm. This range of values is representative of the interplatelet distance measured on several organo-modified lamellar nanofillers[23,24]. The matrix diffusivity was fixed to $D_0 = 10^{-12}$ m²/s while in a second step, the diffusivity in the interplatelet space, denoted by D_{inter}, could be varied in the range [$10^{-4}\ D_0$ – $10^{5}\ D_0$]. Indeed, some experimental works have shown that the interplatelet space within stacks could not always be considered as impermeable[25–27]. It could then be interesting to consider through a parametric analysis a wide range of interplatelet behavior going from very low permeability to high permeability.

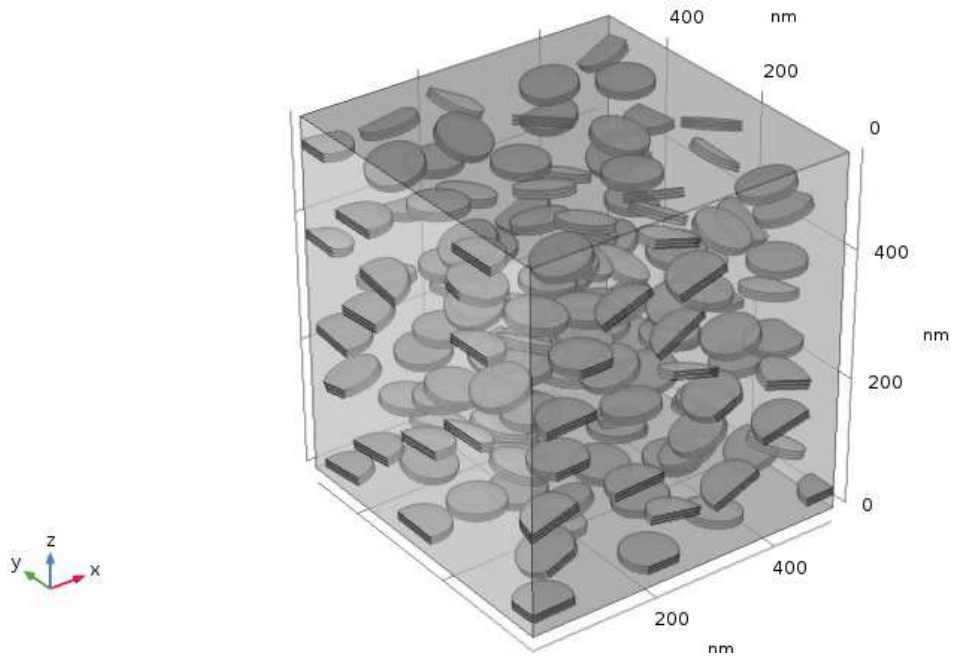

Figure 11 : Geometrical model of intercalated non-oriented monodisperse system

3.2.2.1. Analysis of interplatelet space contribution to overall diffusion for $D_{inter} = D_0$

Several experimental studies available in literature describe intercalated nanocomposite as systems for which interplatelet diffusion inside stacks is considered similar to diffusion in the polymer matrix[18,28,29]. Indeed, Nazarenko et al.[18]showed that for low values of e_{inter} (about 5 nm), intra-stack diffusion can be considered as negligible compared to the overall diffusion. In addition, different analytical and numerical models[19,20,30] investigated the effect of stacks on the barrier properties of intercalated nanocomposite systems. However, the structural parameters appearing in some works were considered over a limited range of values, for example, in Greco et al. work[30], the filler aspect ratio was fixed to 50 however interplatelet space did not exceed 4 nm). Since it was shown in previous works[1,21,31] that the effective diffusivity in nanocomposite systems strongly depends on fillers structural parameters, it appears necessary to extend those analyses to different values.

In order to assess the importance of interplatelet diffusion, a suitable approach consists in comparing the predicted effective diffusivity in identical systems in which the interplatelet space is assumed either permeable ($D_{inter} = D_0$) or impermeable. In the latter case, the stacks can be modeled by the corresponding fully impermeable cylindrical volume, as shown in Figure 12. Note that in both cases, stacks positions are kept strictly identical in order to cancel all variability effects due to random positioning.

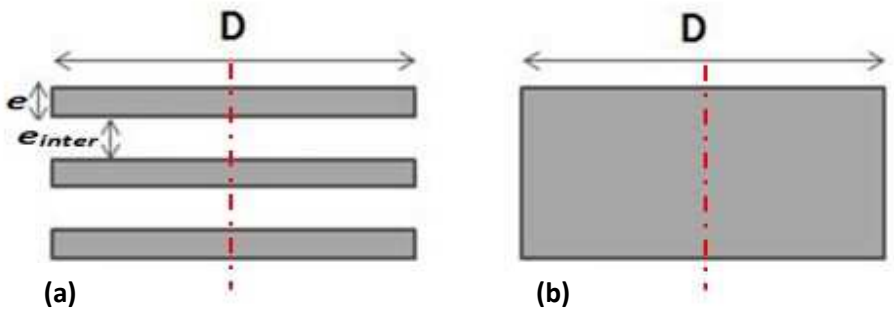

Figure 12 : Geometry of the actual stack **(a)** and corresponding fully impermeable stack **(b)**

The relative effective diffusivity values predicted by the FEM simulations (for a monodisperse size distribution case; D ranging between 20 and 100 nm, e=2nm and f between 0.11 and 2.7%) have been plotted on Figure 13 as a function of the interlayer thickness e_{inter} and of the parameter R which was defined as the ratio of the interplatelet space volume to the total stack volume:

$$\boldsymbol{R = \frac{2e_{inter}}{3e+2e_{inter}}} \qquad (7)$$

As shown by equation 7, the parameter R increases with increasing intra-stacks spacing e_{inter}.

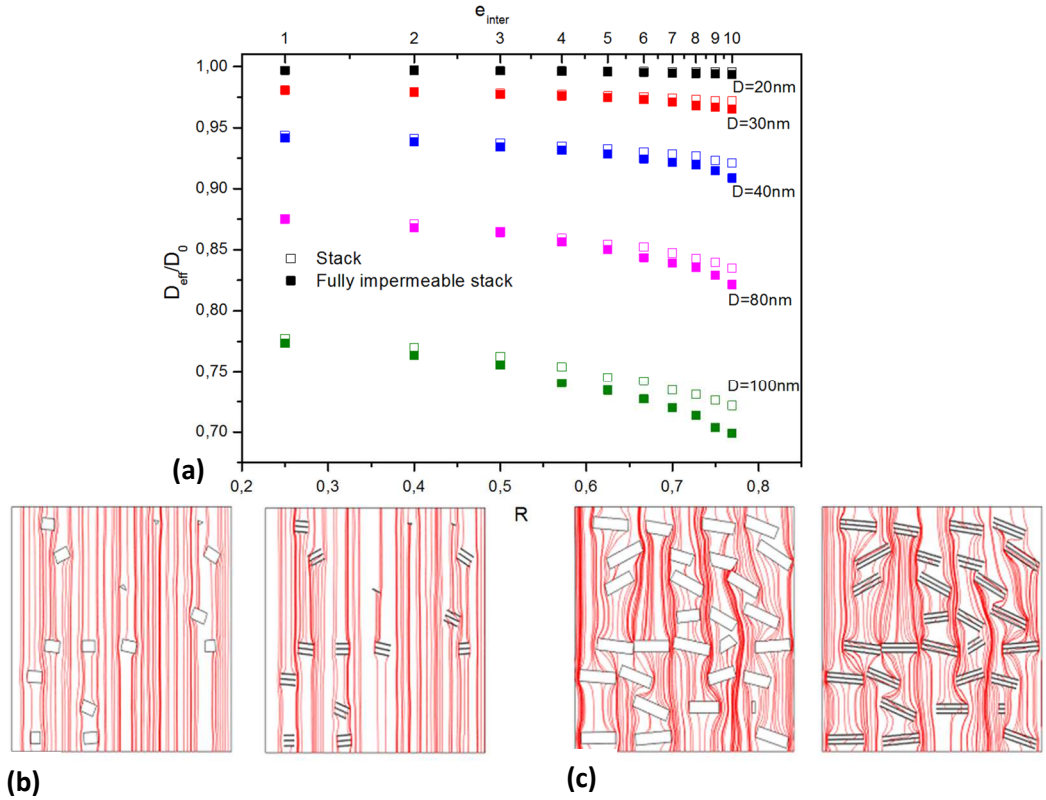

Figure 13: (a) Relative effective diffusivity variation versus parameters R and e_{inter} for systems with permeable stacks (empty symbols) and corresponding fully impermeable stacks (full symbols), for several disk diameter values; **(b)** Diffusive flux lines in system with fully impermeable stacks (left) and permeable stacks (right), D = 20 nm, e_{inter}=7nm; **(c)** Diffusive flux lines in system with fully impermeable stacks (left) and permeable stacks (right), D = 100 nm, e_{inter}=7nm

Fig. 13 shows that for a given volume fraction, the barrier effect is enhanced when R (*i.e.* e_{inter}) is increased. Moreover, the enhancement is more pronounced as the diameter of stacks increases. This result could be explained by the following mechanism: since spacing between stacked fillers increases, the stacks occupy more space in the matrix, which is correlated to a reduction of the free volume and then a decrease in effective diffusivity. Comparing the results for permeable stacks and impermeable stacks leads to the conclusion that interplatelet flux could be neglected if the filler diameter or the interplatelet gap are small. Indeed, the relative effective diffusivity values predicted in the cases of permeable stacks and impermeable stacks remain very close (*e.g.* for R = 0.75 and D = 20 nm, the deviation in relative effective diffusivity values is only 0.18 %). This result is in adequacy with the observations of Nazarenko et al.[18]. The minor contribution of the diffusion in interplatelet spaces to the overall diffusion was confirmed through the analysis of the diffusive flux lines shown in Figure 13(b). However, for large and loosely stacked fillers, intra-stack diffusion can become slightly significant (*e.g.* for R = 0.75 and D = 100 nm, the effective diffusivity increases by 3.3 % if the interplatelet space is permeable). However, this contribution remains low as evidenced by the diffusive lines shown in Figure 13(c) for D=100nm and e_{inter}=7nm. In order to go deeper in the analysis of the influence of e_{inter} on the overall diffusivity, the impact of filler volume fraction has been investigated, for a filler diameter D = 100 nm (Figure 14). Indeed, it has to be noticed from figure 13 (a) that this filler diameter leads to the highest barrier properties.

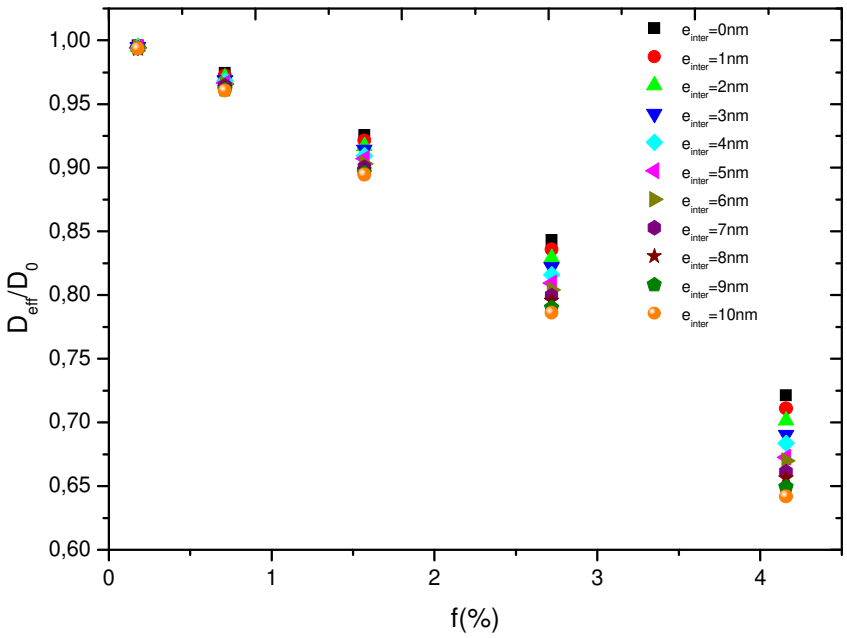

Figure 14 : Relative effective diffusivity variation versus filler volume fraction for several values of interplatelet spacing

The obtained results clearly show that relative effective diffusivity is decreasing when the spacing between fillers in one stack increases, which confirms that diffusion, occurs preferentially in the vicinity of the stacks and not through them. This effect is accentuated for higher fillers volume fractions, since this parameter is known to promote tortuosity in the system. In agreement with previous works[13,14,18,19,30]these observations confirm, for larger ranges of fillers size and interplatelet spacing values, that the contribution of interplatelet spaces to overall diffusion in intercalated systems is actually very limited.

3.2.2.2. Influence of interplatelet diffusivity ($D_{inter} \neq D_0$)

The effect of diffusion inside stacks has been little studied in literature. For instance, Greco et al. [19,20,30]showed that relative effective diffusivity is increasing linearly in function of D_{inter}/D_0 for values ranging between 0.2 and 1.8. We aim to expand D_{inter}/D_0 range to go from nearly impermeable to highly diffusive interplatelet areas. The methodology is similar to that described in section 3.2.2. Fillers volume fraction was varied in the range [0.11% - 2.6%] whereas the intra-stack relative diffusivity D_{inter}/D_0 was varied between 10^{-3} and 10^{5}. Disks diameter was varied between 20 and 100 nm. The predicted evolution of the nancomposites relative effective diffusivity is represented on Fig. 15 versus D_{inter}/D_0.

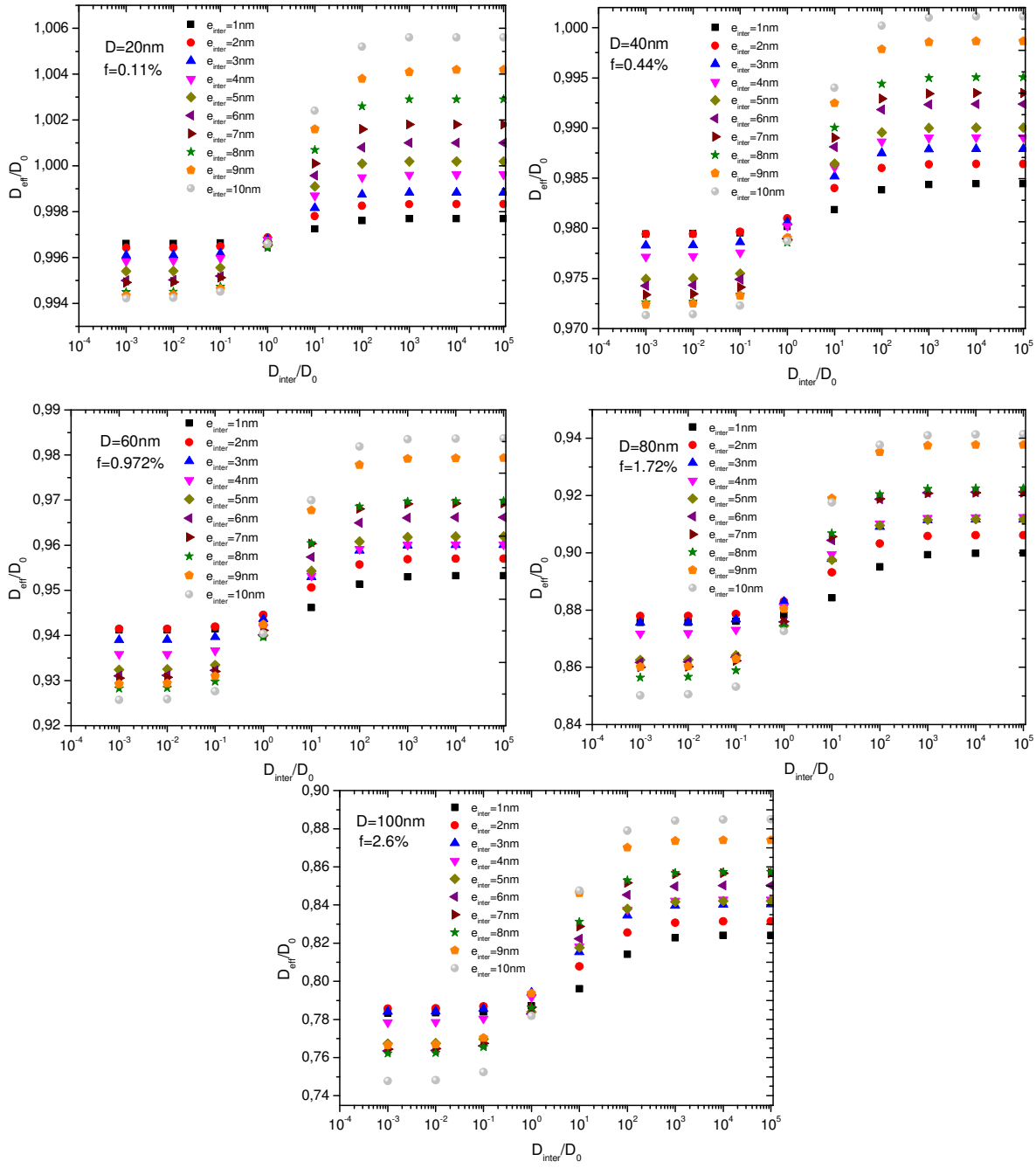

Figure 15: Relative effective diffusivity variation versus D_{inter}/D_0 for several diameter values

First, one should notice that relative effective diffusivity values are decreasing when stacks diameter is increasing which is in agreement with the results discussed in Fig. 13 (a). In addition, three distinct regions are clearly visible in the plots:

- low values of $\frac{\boldsymbol{D_{inter}}}{\boldsymbol{D_0}}$: this region corresponds to the case of nearly impermeable interplatelet spaces, for which the effective diffusivity of the system decreases when spacing between fillers in one stack increases. For each disk diameter (*D),* filler volume fraction (*f)* and interplatelet (e_{inter}), the relative effective diffusivity values define a plateau showing that there is no significant effect of intra-stack diffusivity on the simulated coefficient of diffusion in that region;

- $0.1 < \frac{\boldsymbol{D_{inter}}}{\boldsymbol{D_0}} < 10$: this region corresponds to an interplatelet diffusivity of the same order of magnitude as that of the matrix. The relative effective diffusivity increases as D_{inter}/D_0 increases. Its evolution shows an inflection point which is converging towards lower values when disks diameter and volume fraction increase. This region reveals the significant effect of the interplatelet diffusivity on the nanocomposite effective diffusivity and one must conclude that the barrier effect caused by increasing interplatelet spacing is compensated and even largely exceeded by the intra-stack diffusion effect;

- high values of $\frac{\boldsymbol{D_{inter}}}{\boldsymbol{D_0}}$: this region corresponds to highly diffusing interplatelet spaces, for which the effective diffusivity of the system increases with the interplatelet spacing. In this case, the contribution of interplatelet diffusion becomes very significant. One must see here that all curves are converging to constant values showing that intra-stack diffusivity has, as expected, a local effect and then doesn't affect the overall diffusivity. At last, it can be observed that for D_{inter}/D_0~10, low disks diameters (D=20 nm and D=40 nm) and disks volume fraction values (0.11% and 0.44%), the nanocomposite system is being more permeable than the polymer matrix for large e_{inter} values. This result underlines that in some cases, the presence of stacks can be totally detrimental to barrier properties.

4. Conclusion

In this study, a 3D numerical model of mass diffusion in nanocomposites, based on the Finite Element Method, was built in order to investigate the effects of several key morphological parameters on barrier properties. Different types of disk-shaped fillers, spatial distribution and size dispersion were taken into account in the model. Polydisperse fillers were found to be more efficient than monodisperse fillers for the enhancement of nanocomposites barrier properties, which is more apparent when the size polydispersity is large (Gaussian distribution). Furthermore, the simulations showed that on a given range of filler diameter, uniform (equiprobable) polydispersity is more effective than Gaussian polydispersity. These results were extended and validated in the case of intercalated nanocomposite systems. Accordingly, the developed model predicts that these systems are less efficient than exfoliated systems in the enhancement of barrier properties for an equivalent volume fraction value. Moreover, effective diffusivity was predicted to be strongly dependent on interplatelet spacing within stacks. The results were compared to fully impermeable stack for a large range of parameter values i.e. for large ranges of fillers size and interplatelet spacing values; the contribution of interplatelet spaces to overall diffusion in intercalated systems can be considered as limited when the intra-stack diffusion value is equal or below the matrix diffusivity value. However, it can be detrimental to barrier properties, especially when the platelet diameter is low, the interplatelet distance is important and its diffusivity exceeds that of the matrix by an order of magnitude. The present approach will be enriched in a further work with the study of the presence of an interphase layer which can play a very important role in nanocomposites transport properties.

References

[1] S. Zid, M. Zinet, E. Espuche, 3D Mass diffusion in ordered nanocomposite systems: Finite element simulation and phenomenological modeling, J. Polym. Sci. Part B Polym. Phys. 57 (2019) 51–61. doi:10.1002/polb.24758.

[2] A. Greco, Simulation and modeling of diffusion in oriented lamellar nanocomposites, Comput. Mater. Sci. 83 (2014) 164–170. doi:10.1016/j.commatsci.2013.11.019.

[3] A. Greco, A. Maffezzoli, Two-dimensional and three-dimensional simulation of diffusion in nanocomposite with arbitrarily oriented lamellae, J. Membr. Sci. 442 (2013) 238–244. doi:10.1016/j.memsci.2013.04.038.

[4] M. Minelli, M.G. Baschetti, F. Doghieri, Analysis of modeling results for barrier properties in ordered nanocomposite systems, J. Membr. Sci. 327 (2009) 208–215. doi:10.1016/j.memsci.2008.11.021.

[5] M. Minelli, M.G. Baschetti, F. Doghieri, A comprehensive model for mass transport properties in nanocomposites, J. Membr. Sci. 381 (2011) 10–20. doi:10.1016/j.memsci.2011.06.036.

[6] K. Yano, A. Usuki, A. Okada, T. Kurauchi, O. Kamigaito, Synthesis and properties of polyimide–clay hybrid, J. Polym. Sci. Part Polym. Chem. 31 (1993) 2493–2498. doi:10.1002/pola.1993.080311009.

[7] H.-D. Huang, P.-G. Ren, J.-Z. Xu, L. Xu, G.-J. Zhong, B.S. Hsiao, Z.-M. Li, Improved barrier properties of poly(lactic acid) with randomly dispersed graphene oxide nanosheets, J. Membr. Sci. 464 (2014) 110–118. doi:10.1016/j.memsci.2014.04.009.

[8] L.E. Nielsen, Models for the Permeability of Filled Polymer Systems, J. Macromol. Sci. Part - Chem. 1 (1967) 929–942. doi:10.1080/10601326708053745.

[9] B. Alexandre, D. Langevin, P. Médéric, T. Aubry, H. Couderc, Q.T. Nguyen, A. Saiter, S. Marais, Water barrier properties of polyamide 12/montmorillonite nanocomposite membranes: Structure and volume fraction effects, J. Membr. Sci. 328 (2009) 186–204. doi:10.1016/j.memsci.2008.12.004.

[10] C. Masclaux, F. Gouanvé, E. Espuche, Experimental and modelling studies of transport in starch nanocomposite films as affected by relative humidity, J. Membr. Sci. 363 (2010) 221–231. doi:10.1016/j.memsci.2010.07.032.

[11] E. Picard, J.-F. Gérard, E. Espuche, Water transport properties of polyamide 6 based nanocomposites prepared by melt blending: On the importance of the clay dispersion state on the water transport properties at high water activity, J. Membr. Sci. 313 (2008) 284–295. doi:10.1016/j.memsci.2008.01.011.

[12] H. Kim, A.A. Abdala, C.W. Macosko, Graphene/Polymer Nanocomposites, Macromolecules. 43 (2010) 6515–6530. doi:10.1021/ma100572e.

[13] E. Picard, A. Vermogen, J.-F. Gérard, E. Espuche, Barrier properties of nylon 6-montmorillonite nanocomposite membranes prepared by melt blending: Influence of the clay content and dispersion state: Consequences on modelling, J. Membr. Sci. 292 (2007) 133–144. doi:10.1016/j.memsci.2007.01.030.

[14] N.K. Lape, E.E. Nuxoll, E.L. Cussler, Polydisperse flakes in barrier films, J. Membr. Sci. 236 (2004) 29–37. doi:10.1016/j.memsci.2003.12.026.

[15] X. Chen, T.D. Papathanasiou, Barrier Properties of Flake-Filled Membranes: Review and Numerical Evaluation, J. Plast. Film Sheeting. 23 (2007) 319–346. doi:10.1177/8756087907088437.

[16] R.K. Bharadwaj, Modeling the Barrier Properties of Polymer-Layered Silicate Nanocomposites, Macromolecules. 34 (2001) 9189–9192. doi:10.1021/ma010780b.

[17] D.R. Paul, L.M. Robeson, Polymer nanotechnology: Nanocomposites, Polymer. 49 (2008) 3187–3204. doi:10.1016/j.polymer.2008.04.017.

[18] S. Nazarenko, P. Meneghetti, P. Julmon, B.G. Olson, S. Qutubuddin, Gas barrier of polystyrene montmorillonite clay nanocomposites: Effect of mineral layer aggregation, J. Polym. Sci. Part B Polym. Phys. 45 (2007) 1733–1753. doi:10.1002/polb.21181.

[19] A. Greco, C.E. Corcione, A. Maffezzoli, Effect of multi-scale diffusion on the permeability behavior of intercalated nanocomposites, J. Membr. Sci. 505 (2016) 92–99. doi:10.1016/j.memsci.2016.01.029.
[20] A. Greco, A. Maffezzoli, Finite element simulation and analytical modeling of 3D multi scale diffusion in nanocomposites with permeable stacks, Model. Simul. Mater. Sci. Eng. 24 (2016) 015003. doi:10.1088/0965-0393/24/1/015003.
[21] S. Zid, M. Zinet, E. Espuche, Modeling diffusion mass transport in multiphase polymer systems for gas barrier applications: A review, J. Polym. Sci. Part B Polym. Phys. 56 (2018) 621–639. doi:10.1002/polb.24574.
[22] C.E. Corcione, F. Freuli, A. Maffezzoli, The aspect ratio of epoxy matrix nanocomposites reinforced with graphene stacks, Polym. Eng. Sci. 53 (2013) 531–539. doi:10.1002/pen.23292.
[23] K. Dal Pont, J.F. Gérard, E. Espuche, Modification of α-ZrP nanofillers by amines of different chain length: Consequences on the morphology and mechanical properties of styrene butadiene rubber based nanocomposites, Eur. Polym. J. 48 (2012) 217–227. doi:10.1016/j.eurpolymj.2011.11.006.
[24] D. de M. Mariano, D. de F. da S. Freitas, L.C. Mendes, A.L.F. Carvalho, F.J.H.T.V. Ramos, D. de M. Mariano, D. de F. da S. Freitas, L.C. Mendes, A.L.F. Carvalho, F.J.H.T.V. Ramos, Investigation on Structural, Morphological and Relaxometric Properties of Lamellar Zrp Modified with Long Chain Amine, Mater. Res. 22 (2019). doi:10.1590/1980-5373-mr-2018-0493.
[25] E. Jacquelot, E. Espuche, J.-F. Gérard, J. Duchet, P. Mazabraud, Morphology and gas barrier properties of polyethylene-based nanocomposites, J. Polym. Sci. Part B Polym. Phys. 44 (2006) 431–440. doi:10.1002/polb.20707.
[26] K. Dal Pont, Nanocomposites à matrice élastomère à base de charges lamellaires synthétiques alpha-ZrP : influence de la modification des charges sur les propriétés mécaniques et barrière aux gaz, phdthesis, Université Claude Bernard - Lyon I, 2011. https://tel.archives-ouvertes.fr/tel-00845462/document (accessed April 5, 2019).
[27] C.L. Aitken, W.J. Koros, D.R. Paul, Gas transport properties of biphenol polysulfones, (2002). doi:10.1021/ma00040a008.
[28] R.K. Bharadwaj, A.R. Mehrabi, C. Hamilton, C. Trujillo, M. Murga, R. Fan, A. Chavira, A.K. Thompson, Structure–property relationships in cross-linked polyester–clay nanocomposites, Polymer. 43 (2002) 3699–3705. doi:10.1016/S0032-3861(02)00187-8.
[29] C. Wolf, H. Angellier-Coussy, N. Gontard, F. Doghieri, V. Guillard, How the shape of fillers affects the barrier properties of polymer/non-porous particles nanocomposites: A review, J. Membr. Sci. 556 (2018) 393–418. doi:10.1016/j.memsci.2018.03.085.
[30] A. Greco, A. Maffezzoli, Finite Element Modeling of Multiscale Diffusion in Intercalated Nanocomposites, J. Nanomater. (2015). doi:10.1155/2015/482698.
[31] E.L. Cussler, S.E. Hughes, W.J. Ward, R. Aris, Barrier membranes, J. Membr. Sci. 38 (1988) 161–174. doi:10.1016/S0376-7388(00)80877-7.